The Hippo Signaling Pathway Regulates Corneal Endothelial Regeneration

Jingbin Zhuang, Yuli Guo, Houjian Zhang, Meiqin Zhong, Xu Hu, Lingyu Zhang, Jingwen Yu, Yuqian Wang, Shundong Cai, Huping Wu, Chengchao Chu, Hui He, Rongrong Zong, Weifu Huang, Andrew J. Quantock, Zuguo Liu, Wei Li**

J. Zhuang, Y. Guo, M. Zhong, X. Hu, L. Zhang, J. Yu, Y. Wang, S. Cai, H. Wu, C. Chu, H. He, R. Zong, Z. Liu, W. Li

Xiamen University Affiliated Xiamen Eye Center, Fujian Provincial Key Laboratory of Ophthalmology and Visual Science; Fujian Engineering and Research Center of Eye Regenerative Medicine; Eye Institute of Xiamen University; School of Medicine, Xiamen University; Xiamen, China.

E-mail: Z. Liu, zuguoliu@xmu.edu.cn; W. Li, wei1018@xmu.edu.cn

Y. Guo, H. Zhang, Z. Liu

Department of Ophthalmology, the First Affiliated Hospital of University of South China; Hengyang, Hunan, China.

Z. Liu, W. Li

Department of Ophthalmology, Xiang'an Hospital of Xiamen University, School of Medicine, Xiamen University; Xiamen, China.

W. Huang

TowardPi Medical Technology Beijing; Beijing, China.

A. Quantock

School of Optometry and Vision Sciences, Cardiff University, Cardiff, UK.

Authorship note: J. Zhuang, Y. Guo, and H. Zhang contributed equally to this work and are co-first authors.

Funding: This study was supported in part by the National Natural Science Foundation of China (82471047, 81970773, 82401223), China Post-doctoral science foundation (2024M751351, 2023M741610, BX20240154), Natural Science Foundation of Hunan Province, China (2025JJ90130), Natural Science Foundation of Hunan Province, China (2024JJ6403).

Key words: corneal endothelium, regeneration, Hippo, YAP

Abstract

Corneal endothelial cells (CECs) have limited regeneration capacity in primates while

display a potent restorative capability in some species such as rodents after wounding. The mechanism which determines the regenerative capability of CECs remains poorly understood. Here, we identify that the Hippo signaling pathway is inhibited and the downstream effector YAP is activated during CEC wound healing in rabbit and mouse. Knockdown of *Yap1* and pharmacological inhibition of YAP suppresses CECs wound healing in rodents in both *in vitro* and *in vivo* models. XMU-MP-1, a specific small molecular inhibitor for Hippo signaling pathway, can promote the corneal endothelial regeneration in rodents and corneal endothelial proliferation in cultured primate CECs, as well as *in vivo* non-human primate CEC wounding model. These findings suggest that Hippo pathway serves as a conserved signal to regulate corneal endothelial regeneration among various species, providing a novel target for non-invasive treatment of corneal endothelium decompensation.

1. Introduction

The inner surface of cornea consists a single layer of hexagonal corneal endothelial cells (CECs) which maintain hydration and transparency of cornea through barrier function and pump function of CECs.[1, 2] The normal density of CEC in adult humans is 2500 cells/mm^2 in average.[3] When CEC density falls below a critical threshold around 500 cells/mm^2, the corneal endothelial function will be decompensated, with the result of corneal edema, opacity and progressive vision loss [4, 5], constituting one of the leading causes of corneal blindness.[6]

Currently, surgical treatment is the major therapeutic approach for corneal endothelial decompensation, including Descemet stripping endothelial keratoplasty and Descemet's membrane endothelial keratoplasty.[7, 8] However, it is limited by global shortage of corneal donor tissue. Several researches tried to transplant cultured human CECs [9, 10] and human pluripotent stem cell derived CECs [11] to replenish the lost CECs. A series of studies on animal models [12-15] and clinical trials [16-18] have shown that Rho-kinase inhibitors (ROCKi) could promote CEC wound healing. However, there are currently no pharmaceutical interventions clinically approved for corneal endothelial decompensation.

The regenerative capacity of CEC varies among species. Although CECs in primates exhibit limited *in vivo* proliferation capacity, CECs in rodents such as rabbit and mouse demonstrate a robust ability to regenerate,[19, 20] while underneath mechanism is poorly understood. Over the past few years, tissues from other species possessing regenerative capability have been extensively utilized to study the molecular mechanism, contributing to identification of novel pharmaceutical targets to treat human diseases.[21-23] Therefore, investigating the mechanism of corneal endothelial wound healing in rodents may provide insights for exploring strategies for human corneal endothelial regeneration.

The Hippo pathway has been reported to play a crucial role in tissue wound healing and organ development and regeneration.[24-27] It functions via a phosphorylation cascade involving MST1/2, LATS1/2, and MOB1A/B proteins, which subsequently phosphorylates the downstream transcriptional cofactors YAP/TAZ for their

76 cytoplasmic retention. When the Hippo pathway is inactivated, unphosphorylated
77 YAP/TAZ translocates into the nucleus and initiates transcription of pro-proliferative
78 and pro-survival genes to promote cell regeneration.[28, 29] However, whether this
79 evolutionarily conserved pathway contributes to the regenerative capacity of CECs
80 remains unknown. In this study, we investigated the role of Hippo signaling pathway
81 on corneal endothelial wound healing and determined whether this signaling pathway
82 can be a regulator of corneal endothelial regeneration in multiple species.
83

84 **2. Results**

85 **2.1 Hippo-YAP pathway changes during corneal endothelial wound healing**

86 To determine whether the Hippo-YAP signaling axis is engaged in CEC wound
87 healing, we investigated the status of Hippo pathway during CEC wound healing
88 across species using a rabbit CEC cryoinjury model (**Figure 1**A), a mouse ultraviolet
89 (UV)-induced CEC damage model (Figure 1E), and an *in vitro* primary monkey CEC
90 scraping model (Figure S1A, Supporting Information). YAP phosphorylation was
91 significantly decreased on day 7 and returned to baseline level on day 14 after CEC
92 cryoinjury in rabbit (Figure 1B,C). Phosphorylated MST1 and LATS1, two key
93 kinases in the Hippo pathway, showed similar pattern (Figure 1B,C). There was
94 obvious YAP nuclear translocation on day 7 compared to day 0 and day 14 (Figure
95 1D), indicating the activation of YAP. Similar finding was also detected during wound
96 healing of UV-induced mouse CEC damage (Figure 1F) and the primary monkey
97 CEC scraping model (Figure S1B,C, Supporting Information). Collectively, these
98 results indicated that the Hippo pathway was downregulated and YAP was activated
99 during CEC wound healing in different species.

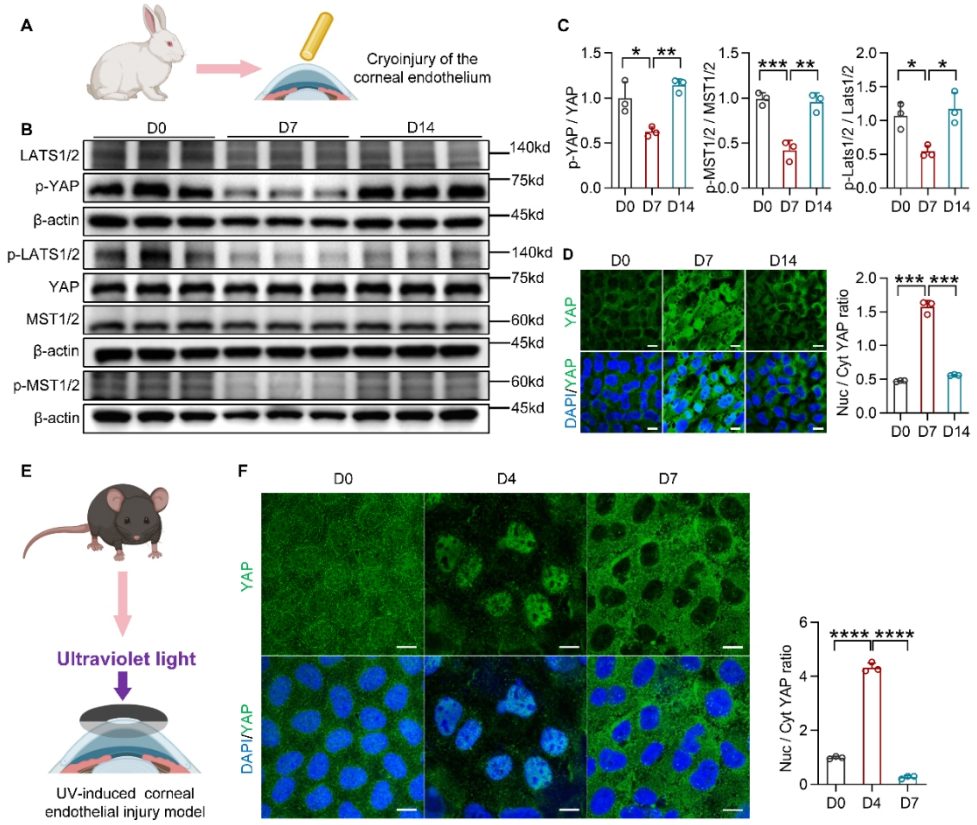

Figure 1. Downregulation of Hippo pathway and YAP activation during CEC wound healing. (A) The diagram shows the rabbit corneal endothelial injury model. (B, C) Western blot analysis of p-YAP, YAP, p-MST1/2, MST1/2, p-LATS1/2, LATS1/2 and β-actin, the protein levels were quantified by densitometry (n=3). (D) Representative immunofluorescence images of YAP in rabbits and the ratio of nuclear YAP to cytoplasm YAP, five cells were randomly selected for measurement and averaged in each sample (n = 3). (E) The diagram shows the mouse corneal endothelial injury model. (F) Representative immunofluorescence images of YAP in mice and the ratio of nuclear YAP to cytoplasm YAP, five cells were randomly selected for measurement and averaged in each sample (n = 3). *P < 0.05, **P < 0.01, ***P < 0.001, ****P < 0.0001, error bars, mean ± SEM. Scale bars represent 10 μm in (D) and (F). Nuc, nucleus; Cyt, cytoplasm.

2.2 Hippo pathway is a major regulator of CEC regeneration

To further elucidate the role of Hippo pathway in CEC regeneration, we applied verteporfin, a specific inhibitor of YAP which disrupts the YAP-TEAD interaction,[30]

116 to block YAP function. EdU labeling and Ki67 staining showed reduced proliferation
117 of primary rabbit CECs under verteporfin treatment (**Figure 2**A). CCK8 assay
118 showed that verteporfin inhibited viability of primary rabbit CECs in a
119 dose-dependent manner (Figure 2B). Human CEC line B4G12 demonstrated similar
120 changes after YAP inhibition (Figure S2, Supporting Information). Verteporfin eye
121 drops were subsequently administrated to treat rabbits following corneal endothelial
122 cryoinjury, and the cornea showed reduced transparency on day 7 and cloudy central
123 cornea on day 13 (Figure 2C,F). Anterior segment optical coherence tomography
124 (OCT) examination showed delayed recovery of corneal edema in verteporfin treated
125 rabbit (Figure 2D,F). Alizarin red staining of rabbit corneas on day 13 confirmed
126 delayed CEC wound healing after verteporfin application, characterized by absence of
127 cellular structure in the central corneal endothelium (Figure 2E). Similar results were
128 observed in mouse with UV radiation induced corneal endothelial damage (Figure
129 2G-J). Putting together, pharmacological YAP inhibition suppressed the regeneration
130 of CECs in both *in vitro* and *in vivo* models across species.

131 To further confirm the function of YAP in corneal endothelium, primary rabbit
132 CECs were transfected with a siRNA specific to *Yap1*. EdU and Ki67 positive cells
133 were significantly reduced after knockdown of *Yap1* (Figure 2K,L,N). Cell viability
134 was also reduced after knockdown of *Yap1* as measured by CCK8 assay (Figure 2M).
135 Similar results were observed in B4G12 cell line (Figure S3, Supporting Information).
136 Next, we determined the effect of *Yap1* knockdown on wound healing in a mouse
137 model. The adeno-associated virus (AAV) vector carrying *Yap1*-specific short hairpin
138 RNA (AAV-*Yap1*-shRNA) was injected into mouse anterior chamber and verified by
139 ZsGreen expression in the corneal endothelium 4 weeks after injection (Figure 2O).
140 *Yap1* mRNA expression was suppressed in the corneal endothelium of
141 AAV-*Yap1*-shRNA mice (Figure 2P), and the mice showed a delayed recovery from
142 corneal opaque and stromal edema after UV radiation damage (Figure 2Q,R,T). Taken
143 together, pharmacological YAP inhibition and *Yap1* knockdown significantly
144 suppressed corneal endothelial regeneration, supporting the function of Hippo
145 signaling pathway in corneal endothelial wound healing.

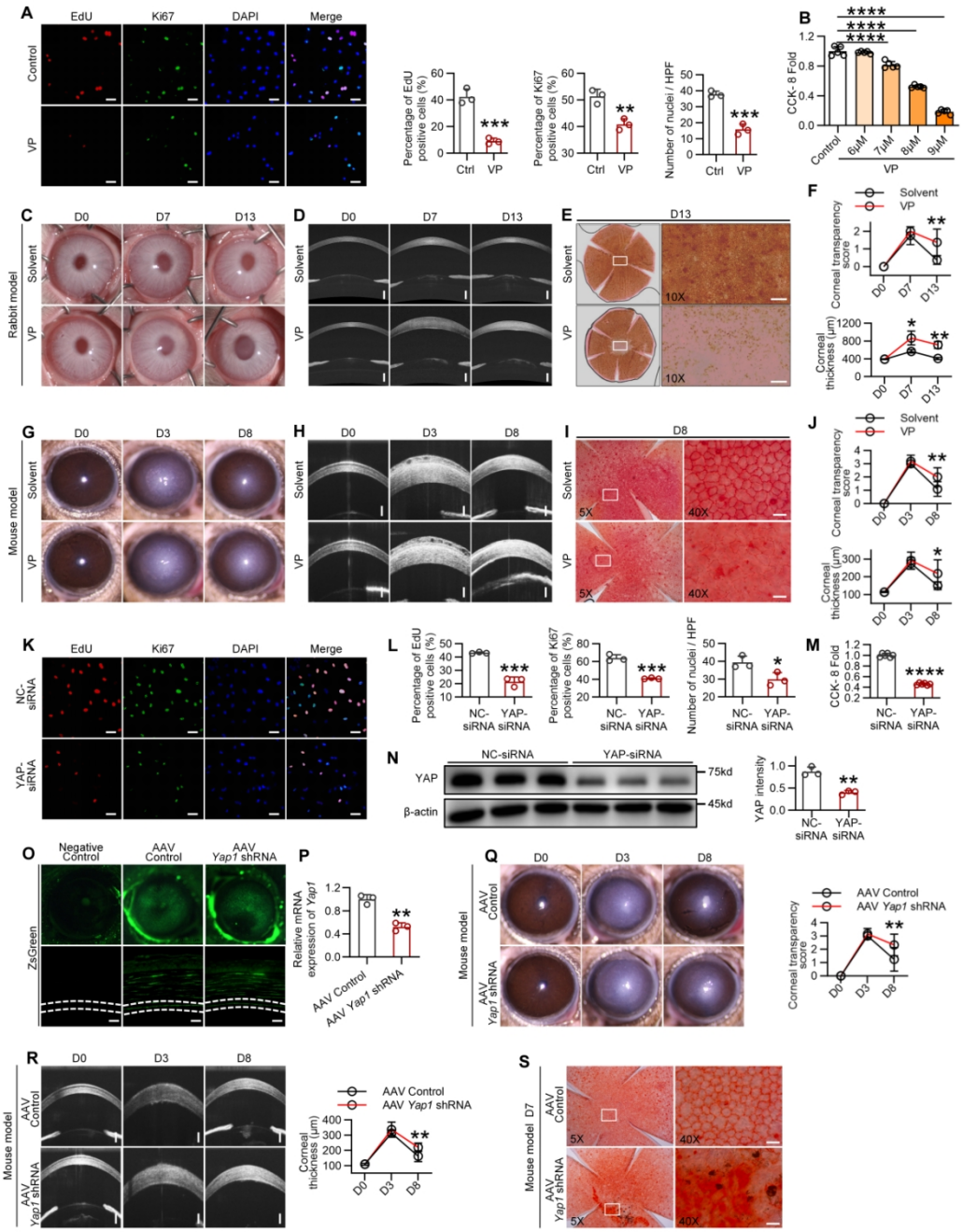

146

147 **Figure 2. Pharmacological YAP inhibition and knockdown of Yap1 suppressed CEC**
148 **regeneration.** (A) Representative staining images of primary rabbit CECs and percentage of
149 EdU and Ki67 positive cells and counting of DAPI (n = 3). (B) CCK-8 assay of primary
150 rabbit CECs. (C to E) Representative slit-lamp images (C), anterior segment OCT images (D)
151 and corneal alizarin red staining images (E) of rabbits. (F) Corneal transparency score and
152 central corneal thickness of rabbits (n = 4). (G to J) Representative images (G to I) and
153 corneal transparency score and central corneal thickness of mouse models (n = 5) (J). (K and

154 L) Representative images (K) of EdU and Ki67 and percentage of EdU, Ki67 positive cells
155 and counting of DAPI (n = 3) (L). (M) CCK-8 assay of primary rabbit CECs. (Fold of control,
156 n = 6). (N) Western blot analysis of YAP in primary rabbit CECs (n = 3). (O) ZsGreen
157 expression in vivo and in corneal sections. (P) Relative mRNA expression of Yap1 in mice
158 corneal endothelium (n = 3). (Q) Representative slit-lamp images and corneal transparency
159 score of mice (n = 6). (R) Representative anterior segment OCT images and central corneal
160 thickness of mouse models (n = 6). (S) Representative corneal alizarin red staining images of
161 mice. *P < 0.05, **P < 0.01, ***P < 0.001, ****P < 0.0001, error bars, mean ± SEM. Scale
162 bars represent 500 μm in (D), 200 μm in (E), 100 μm in (H and R), 50 μm in (A and K), 25
163 μm in (O), and 20 μm in (I and S). VP, verteporfin.

164

165 **2.3 Pharmaceutical inhibition of Hippo pathway with XMU-MP-1 promotes**
166 **CEC regeneration**

167 XMU-MP-1, a specific MST1/2 inhibitor,[31] can block Hippo pathway and restrain
168 the phosphorylation of YAP. We applied XMU-MP-1 in primary rabbit CEC culture
169 and found it can reduce YAP phosphorylation and enhance YAP nuclear translocation
170 in rabbit CECs (Figure S4A,C,E,F, Supporting Information). Additionally,
171 XMU-MP-1 increased EdU and Ki67 positive cells in both rabbit CECs (**Figure 3**A,B)
172 and human B4G12 cell line (Figure S5A-D), and enhanced the cell viability (Figure
173 3C, Figure S5E, Supporting Information). Cell cycle analysis revealed a significant
174 decrease of cells in G1-phase and increase of cells in G2/M-phase after XMU-MP-1
175 application (Figure S6A,B, Supporting Information). XMU-MP-1 treatment also
176 upregulated the expression of cell cycle-related genes including E2F1, CCND1,
177 CCND3, CCNA2 and CCNE1 (Figure S6C,D, Supporting Information).

178 Furthermore, XMU-MP-1 was topically applied in corneal endothelial wound
179 models and found it expedited corneal endothelial wound healing and corneal edema
180 recovery in both rabbits (Figure 3D-G) and mice (Figure 3H-K). Immunostaining
181 revealed that XMU-MP-1-treated mouse corneas showed more contiguous ZO-1
182 (Figure 3L,N) and increased Na^+/K^+-ATPase (Figure 3M,O) expression. Additionally,
183 more EdU-positive cells were found in the corneal endothelium of XMU-MP-1
184 treated mice (Figure 3P). These results indicated that XMU-MP-1 could promote CEC
185 regeneration and functional restoration.

To verify whether XMU-MP-1 can penetrate the cornea, liquid chromatography-tandem mass spectrometry analysis was utilized to assay the concentration of XMU-MP-1 in the rabbit corneal endothelium 1 hour after topical application, and 2974.44 ± 17.43 ng/g of XMU-MP-1 was detected (Figure S7A, Supporting Information). The nuclear translocation of YAP in mouse CECs was also observed following administration of XMU-MP-1 (Figure S7B, Supporting Information).

We further evaluated the ocular manifestation after 4 weeks topical administration of XMU-MP-1 in normal mice. No corneal limbal neovascularization, corneal epithelial defect or corneal thickness changes were observed after XMU-MP-1 application (Figure S8A,B, Supporting Information). There was also no evidence of abnormal tissue proliferation in the conjunctiva, Meibomian glands, or lacrimal glands (Figure S8C, Supporting Information). Additionally, there was no significant difference in tear production, intraocular pressure, axial length, or refraction (Figure S8D-G, Supporting Information) compared with that of the control group. There was also no abnormal retinal thickening or neovascularization detected after XMU-MP-1 application (Figure S8H,I, Supporting Information).

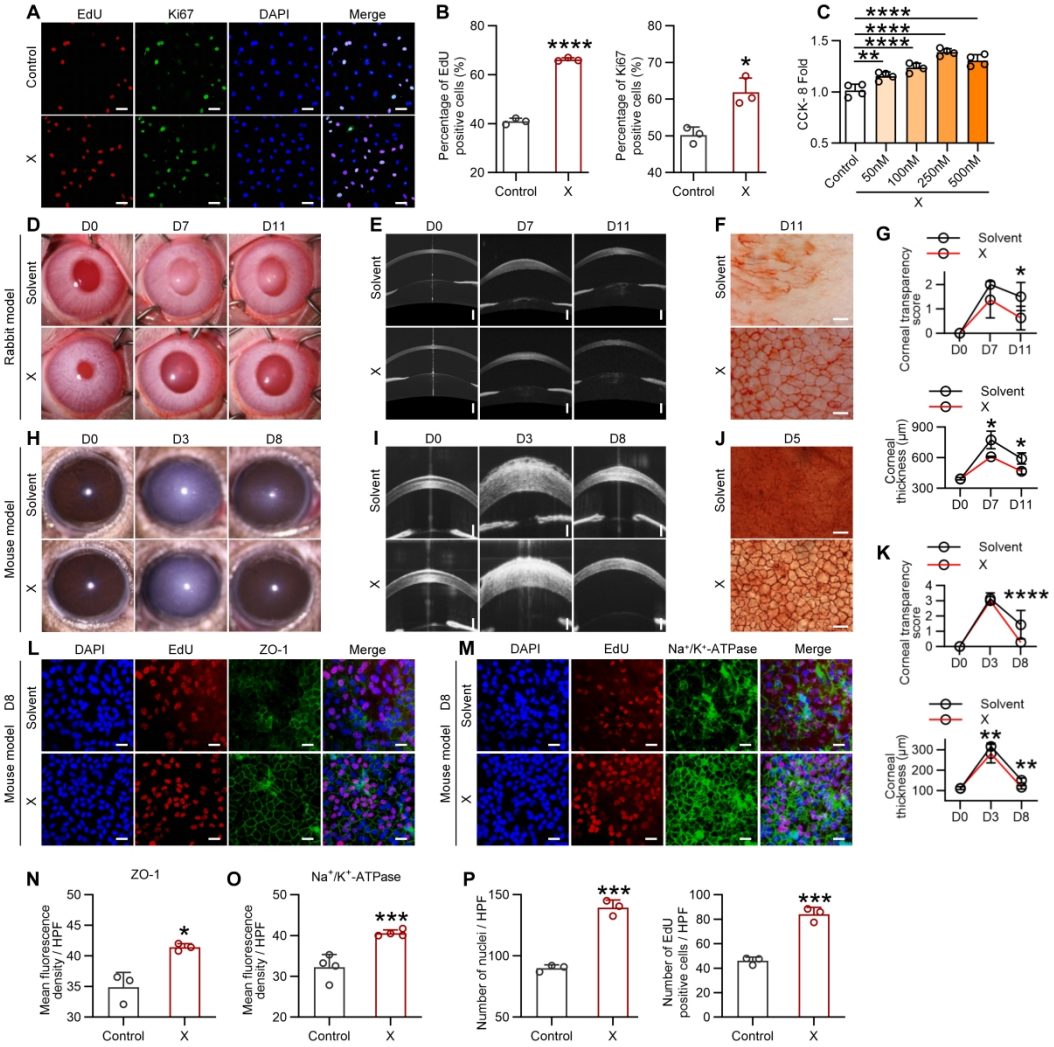

Figure 3. XMU-MP-1 promotes CEC regeneration in rabbit and mouse models. (A and B) Representative staining images of primary rabbit CECs and percentage of EdU and Ki67 positive cells (n = 3). (C) CCK-8 assay of primary rabbit CECs (fold of control, n=4). (D to G) Representative images (D to F) and corneal transparency score and central corneal thickness of rabbit models (n = 3) (G). (H to K) Representative images (H to J) and corneal transparency score and central corneal thickness of mouse models (n = 6) (K). (L and M) EdU staining and immunofluorescence of ZO-1 (L), Na^+-K^+ ATPase (M) of corneal endothelial whole mount. (N and O) The intensities of ZO-1 (N) and Na^+-K^+ ATPase (O) (n = 3). (P) Quantification of EdU positive cells and nuclei counting in (L and M) (n = 3). *P < 0.05, **P < 0.01, ***P < 0.001, ****P < 0.0001, error bars, mean ± SEM. Scale bars represent 500 μm in (E), 100 μm in (I), 50 μm in (A), 25 μm in (L and M) and 20 μm in (F and J). X,

215 XMU-MP-1; ip, intraperitoneal injection.

216

217 **2.4 XMU-MP-1 promotes CEC regeneration in primates**

218 To investigate the effect of XMU-MP-1 on primate CECs, we firstly treated the
219 primary cultured human CECs (**Figure 4**A,B) and monkey CECs (Figure 4C,D) with
220 XMU-MP-1. The results showed that EdU-positive and Ki67-positive cells in both
221 types of CECs increased with XMU-MP-1 administration. Nuclei counting confirmed
222 higher cell density in XMU-MP-1 treated groups despite equal seeding densities
223 (Figure 4A-D). Next, the XMU-MP-1 treatment was applied to an *ex vivo* monkey
224 corneal endothelial scraping model. Trypan blue staining demonstrated that
225 XMU-MP-1 promoted monkey CEC wound healing, with the defect area completely
226 healed by day 4 post scraping (Figure 4E,F).

227 Next, XMU-MP-1 solution was topically applied in cynomolgus monkey after
228 cryoinjury of the central corneas. The slit lamp microscopy (Figure 4G,J) and anterior
229 segment OCT examination (Figure 4H,K) showed that the corneal transparency and
230 thickness restored to normal in XMU-MP-1 treated eyes at week 3, while one control
231 cornea remained obvious opacity and edema. CECs were observed under in vivo
232 confocal microscopy and regular cell morphology was observed 3 weeks after topical
233 application of XMU-MP-1 (Figure 4I). CECs density in the central cornea was
234 restored to pre-injury level with XMU-MP-1 treatment, while it was about half of
235 pre-injury level in control eyes (Figure 4L). These findings suggest that XMU-MP-1
236 effectively promotes CEC regeneration in non-human primates.

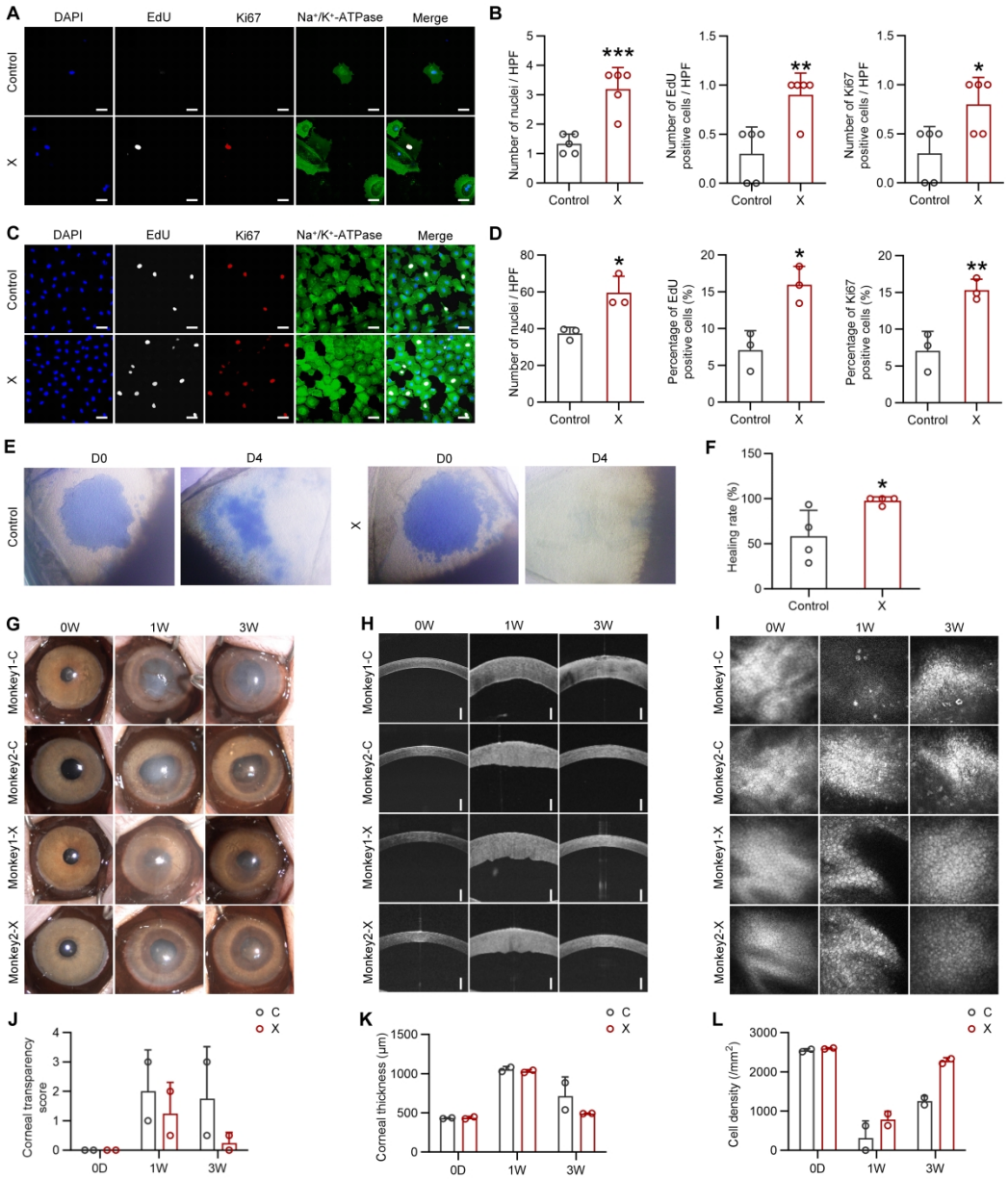

Figure 4. XMU-MP-1 promotes CEC regeneration in non-human primate. (A) EdU and DAPI staining and immunofluorescence of Ki67, Na^+-K^+ATPase in primary human CECs. (B) Nuclei counting and percentage of EdU and Ki67 positive cells in (A) (n = 5). (C) EdU and DAPI staining and immunofluorescence of Ki67 and Na^+-K^+ ATPase in primary monkey CECs. (D) Nuclei counting and percentage of EdU and Ki67 positive cells in (C) (n = 3). (E and F) Trypan blue staining of monkey corneal endothelium explants and the healing rate quantified by stained area (n=4). (G to I) Slit-lamp images (G), anterior segment OCT images (H) and corneal endothelial in vivo confocal microscope graphs (I) of monkeys. (J to L) Corneal transparency score (J), central corneal thickness (K) and central CECs density (L) of

247 monkeys (n=2). *P < 0.05, **P < 0.01, ***P < 0.001, ****P < 0.0001, error bars, mean ±
248 SEM. Scale bars represent 500 μm in (H) and 25 μm in (A and C). C, control; X,
249 XMU-MP-1.

250

251 We further conducted a 12-month follow-up in one monkey after 3-weeks
252 XMU-MP-1 treatment. Slit-lamp examination revealed clear cornea in XMU-MP-1
253 treated eye, while the solvent-treated control eye exhibited stromal opacification
254 (**Figure 5**A). Corresponding anterior segment OCT confirmed lower corneal
255 thickness in XMU-MP-1-treated eye, compared with that of control eye (Figure 5B).
256 In vivo confocal microscopy demonstrated visible, regularly arranged CECs in
257 XMU-MP-1-treated eye, while CECs were undetectable in control eye (Figure 5C).
258 Alizarin red staining further revealed a confluent endothelial monolayer with uniform
259 hexagonal morphology in XMU-MP-1-treated cornea, compared to sparse, irregular
260 cells in control eye (Figure 5D). Additionally, CECs showed integral expression and
261 organized localization of Na^+/K^+-ATPase and ZO-1 in treated cornea, while control
262 cornea displayed disorganized expression of both markers (Figure 5E). Collectively,
263 these results demonstrate that a short-term XMU-MP-1 treatment promoted corneal
264 endothelial regeneration after wounding, and the structure and function of corneal
265 endothelium could be maintained over an extended period without further therapeutic
266 intervention.

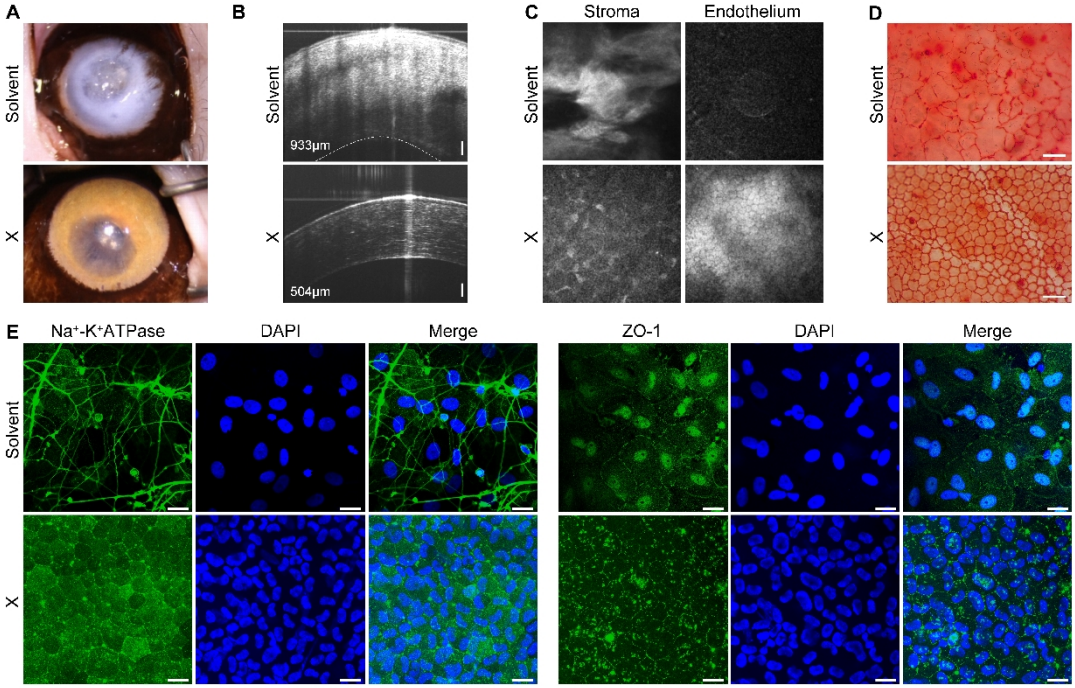

Figure 5. Long-term follow-up on monkey corneal endothelium transiently treated with XMU-MP-1 post-injury. (A to C) Representative slit-lamp images (A), anterior segment OCT images (B) and in vivo confocal microscope graphs (C) of XMU-MP-1-treated eye and the solvent control eye at 12 months after treatment cessation. (D) Alizarin red staining of monkey corneal endothelium. (E) Immunofluorescence staining of Na^+/K^+-ATPase and ZO-1 in monkey corneal endothelium. Scale bars represent 100 μm in (B), 40 μm in (D), and 25 μm in (E). X, XMU-MP-1.

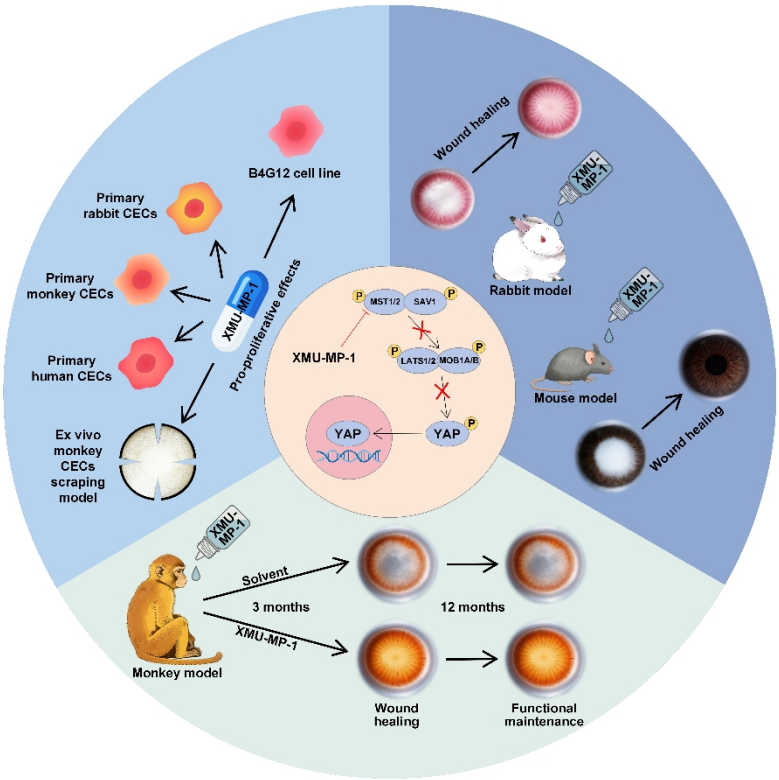

Figure 6. The cross-species pro-regenerative effect of XMU-MP-1. XMU-MP-1-induced activation of YAP promotes proliferation in B4G12 cells, primary rabbit CECs, monkey CECs and human CECs, and accelerates wound healing of *ex vivo* monkey corneal endothelium. XMU-MP-1 also demonstrates robust efficacy in promoting CECs regeneration in rabbit, mouse, and monkey.

3. Discussion

In this study, we identified the activation of Hippo-YAP signaling axis during CEC wound healing and confirmed its regulatory role in CEC regeneration. Hippo pathway inhibitor exhibited efficacy in promoting CEC regeneration across mouse, rabbit and monkey corneal endothelial wounding models (**Figure 6**), indicating the potential of its clinical application in treating corneal endothelial decompensation.

For decades, how to regenerate human CECs has remained a huge challenge. Previous studies have demonstrated that nuclear translocation of YAP is associated with proliferation in primary culture of human CECs,[32, 33] exogenous YAP could induce cell proliferation in contact-inhibited human CECs monolayers.[34] However,

292 the role of the Hippo pathway in CEC regeneration in vivo remains unknown. Our
293 results derived in multi-species in vivo demonstrated that CECs regeneration is
294 regulated by the Hippo pathway. In mouse corneal endothelial wounding model,
295 EdU-positive cells were presented at the margin of injured region on day 3 post injury
296 and expanded to nearly the entire damaged region on day 8 (Figure S9A, Supporting
297 Information). Nevertheless, no EdU-positive cells were observed in the peripheral
298 corneal endothelium (Figure S9A, Supporting Information) and the uninjured corneal
299 endothelium (Figure S9B, Supporting Information), indicating the wound healing
300 process initiates in the CECs at the wound margin, and the cell regeneration process is
301 associated with the inactivation of Hippo pathway. Thus we speculate that the
302 inability of human CECs to regenerate may due to evolutionary loss of the capacity to
303 block the Hippo pathway following injury, a capacity which is retained in rodents.

304 Notably, YAP activation is also associated with endothelial-to-mesenchymal
305 transition (EndMT),[6] a pathological process during CEC wound healing
306 characterized by upregulation of fibroblast biomarkers.[35] Our previous study has
307 found that rabbit CECs underwent a transient fibrotic EndMT following injury, and
308 reversed back to an endothelial phenotype upon completion of wound healing.[35] In
309 this study, YAP activation has been demonstrated to promote cell cycle progression of
310 CECs, and the CECs morphology could be restored to relatively normal state over
311 time, concomitant with functional recovery of the corneal endothelium (Figure S10,
312 Supporting Information). Therefore, EndMT may be also involved in the wound
313 healing of CECs that regulated by YAP.

314 Although XMU-MP-1 has been shown to effectively promote corneal endothelial
315 regeneration, potential side effects arising from YAP activation[36] should be carefully
316 considered. Our evaluation demonstrated that XMU-MP-1 exhibited ocular safety in
317 mice following 4 weeks of topical administration (Figure S8, Supporting Information).
318 Besides XMU-MP-1, TRULI and DMX-5804 are also pharmaceutical inhibitors for
319 the Hippo pathway, which inhibit LATS1/2[37] and non-canonical Hippo pathway
320 MAPK4Ks[38], respectively. In our study, topical administration of TRULI and
321 DMX-5804 also showed effects in promoting CEC proliferation in vitro and in vivo
322 (Figure S11, Supporting Information).

323 In the monkey experiments, we observed lower cell density and obviously irregular
324 cell morphology in central corneal endothelium of the control group. Although one
325 control cornea restored transparency 3 weeks post injury, which may be due to

326 functional compensation of the surviving CECs, the CEC density of that control
327 cornea did not restore to normal level. In comparison, XMU-MP-1 treatment restored
328 both the cell density and morphology of central CECs to near normal levels,
329 demonstrating the efficacy of XMU-MP-1 in promoting primate CECs regeneration.
330 Based on the results obtained from the control group, it is reasonable to suspect that
331 monkey CECs also possess a weak regenerative capacity in vivo, which is not
332 identical to that of human. Given the difference between animal models and clinical
333 conditions, future clinical study is necessary.

334 Our finding that a transient treatment with XMU-MP-1 can restore wounded
335 corneal endothelium in non-human primates highlights a principle in regenerative
336 biology: a properly timed signal modulation can initiate a complete program of tissue
337 repair that extends the duration of the stimulus[39-41]. This contrasts with many chronic
338 degenerative conditions that require prolonged pharmacological management. In the
339 cornea endothelium, the injury itself may create a permissive microenvironment
340 through changes in cell density, mechanical tension or extracellular matrix
341 composition that allows a short pulse of YAP activation to drive not only proliferation
342 but also the subsequent steps of polarity establishment, junctional reassembly, and
343 functional maturation. Once a continuous monolayer of corneal endothelium is
344 restored, contact inhibition and normalized cell-matrix signaling likely reactivate the
345 Hippo pathway, thereby terminate the proliferative phase and preventing over-growth.
346 This built-in feedback mechanism underscores the feasibility of targeting Hippo
347 signaling in corneal endothelium.

348

349 **4. Conclusion**

350 In summary, we identified the Hippo signaling pathway as a regulator for CEC
351 regeneration. Pharmaceutical inhibition of the Hippo pathway promotes corneal
352 endothelial proliferation in multiple corneal endothelial wounding models across
353 species, highlighting its potential for the treatment on corneal endothelial
354 decompensation.

355

356 **5. Methods**

357 *Preparation of compounds:* The solvent for XMU-MP-1 (MCE, HY-100526) and
358 verteporfin (MCE, HY-B0146) consisted of 5% dimethyl sulfoxide (DMSO, MCE,
359 HY-Y0320C), 20% polyethylene glycol 300 (PEG300, MCE, HY-Y0873) and 75%

360 phosphate buffered solution (PBS, Solarbio, P1020).
361 *Animal:* All animals, regardless of gender, were housed in Xiamen University
362 Laboratory Animal Center and maintained under a 12-h light/dark cycle, free access
363 to water and food. Animals used in this study were treated in accordance with the
364 ARVO Statement for the Use of Animals in Ophthalmic and Vision Research.
365 *Animal examination:* Corneal images were obtained using the slit-lamp microscope
366 (TAKAGI, 700GL) and high-definition camera (Canon, EOS 7D). Anterior segment
367 OCT images of rabbits and monkeys were obtained by swept-source OCT (TowardPi,
368 Yalkaid YG-100K) and Small Animal Retina Imaging System (Optoprobe) was used
369 for mice. A laser-scanning in vivo confocal microscope with a corneal imaging
370 module (Heidelberg, HRT3-RCM) was used to observe the central CECs of monkeys,
371 and the method of cell counting refers to our previous study.[42]
372 *Cynomolgus monkey corneal endothelial wound model:* Central corneal endothelium
373 damage was performed using transcorneal cryogenic method as previously
374 described.[43] The corneal endothelium of two cynomolgus monkeys was damaged
375 under general anesthesia by transcorneal freezing with a 5-mm-diameter probe for 20
376 seconds. Before freezing, the copper probe was immersed in liquid nitrogen for 3
377 minutes to stabilize its temperature at approximately -196℃.
378 To evaluate the effect of XMU-MP-1 on CECs wound healing, XMU-MP-1 (50
379 μM) was topically applied to the right eye of each animal 4 times daily for 3 weeks.
380 Solvent was applied to the lateral eye as a control. The experiments on two eyes were
381 conducted separately to avoid affecting the monkeys in their daily activities.
382 *Rabbit corneal endothelial wound model:* The corneal endothelium of New Zealand
383 white rabbits was damaged under general anesthesia by transcorneal freezing with a
384 6-mm-diameter probe for 15 seconds. XMU-MP-1 (50 μM) or verteporfin (50 μM)
385 was topically applied to rabbit eyes 4 times daily after corneal endothelial wounding.
386 For the control group, solvent was administrated.
387 *Mouse corneal endothelial wound model:* The UV-induced mouse corneal endothelial
388 injury was performed as previously reported with modification.[44] In brief, a UVB
389 LED light source (Spectronics Corporation, EB-160C) with an emission peak of 312
390 nm light, 40 nm bandwidth and irradiance of 620 μW/cm^2 was focused to illuminate a
391 2-mm-diameter spot onto the mouse cornea for 7 min with the total irradiance energy
392 of 260.4 J/cm^2. After irradiation, 2 μl of XMU-MP-1 (1 μM) or verteporfin (50 μM)

was topically applied to mouse eyes 4 times daily, and solvent was applied to the control group.

AAV injection in mouse: The AAV was manufactured by Hanbio Biotechnology (Shanghai, China). To achieve endothelial-selective gene knockdown, sequence encoding shYap1 or negative control sequence was constructed under Tie1 promoter and expressed in AAV (Table S1). The virus titer was 1.6×10^{12} μg/ml.

Then, 8-week-old C57BL/6 mice were anesthetized and anterior chamber was injected with AAV Control-ZsGreen or AAV Yap1 shRNA-ZsGreen (3 μl per eye) using a 34-gauge needle. ZsGreen expression was detected in vivo using stereo fluorescence microscope (Leica, M165FC) 4 weeks after injection, then the mice were used to generate corneal endothelial wound model.

Evaluation of corneal transparency: The cornea was observed under slit-lamp microscope and the corneal transparency was evaluated with scores ranged from 0 to 4 as previously reported: 0, a normal cornea; 0.5, a slight haze visible only under a slit-lamp microscope; 1, a mild haze; 2, a moderate haze with a visible iris; 3, a severe haze with an invisible iris; and 4, a severe haze with corneal ulceration.[45]

Ex vivo monkey corneal endothelial scraping model: Two monkey corneas were divided into 12 equal pieces. After culturing for 24 hours with the endothelial surface facing upward, CECs were scraped off within a 2 mm diameter area using a soft rubber rod. Trypan blue staining was used to visualize areas of endothelial defect. The corneal explants were cultured in Dulbecco's Modified Eagle Medium/Nutrient Mixture F-12 (DMEM/F12, Gibco, 11320033) supplemented with 5% fetal bovine serum (FBS, ABW, AB-FBS-0050), 0.5% DMSO, 2 ng/mL mouse EGF (Gibco, PMG8041), 1% Insulin-Transferrin-Selenium-Ethanolamine (ITS-X, Gibco, A4000046401), 0.5 μg/mL hydrocortisone (Yeasen, 54576ES03) and 1% penicillin/streptomycin (P/S, Gibco, 15140-122), with culture medium changed every other day.

Isolation and primary culture of monkey CECs: Monkey CECs were isolated through Descemet's stripping and digestion with 1 mg/mL collagenase A (Merck, 10103578001) for 6 h at 37℃. After 5 min in TrypLE (Thermo Fisher Scientific, 12605010) at 37℃, CECs were pelleted at 1200 rpm for 5 min and plated on fibronectin coating mix (AthenaES, 0407) treated wells. The cells were cultured in Dulbecco's Modified Eagle Medium (DMEM, Gibco, 11965092) with 10% FBS at

426 37°C in 5% CO_2.

427 *Isolation and primary culture of human CECs and rabbit CECs:* Human tissue was
428 handled according to the Declaration of Helsinki. Corneoscleral tissues from human
429 donor eyes were obtained from the Eye Bank of Xiamen Eye Center of Xiamen
430 University immediately after the central corneal button had been used for corneal
431 transplantation. Human CECs and rabbit CECs were isolated using our previous
432 method,[46] and the cells were cultured in DMEM/F12 supplemented with 5% FBS,
433 0.5% DMSO, 2 ng/mL mouse EGF, 1% ITS-X, 0.5 μg/mL hydrocortisone and 1%
434 P/S.

435 *Transfection of rabbit CECs and B4G12 with siRNA:* YAP expression was knocked
436 down in rabbit CECs and B4G12 cell line by transfection with the YAP siRNA
437 (Sangon Biotech) using RNATransMate (Sangon Biotech, E607402) following the
438 manufacturer's instruction, with negative control (NC) siRNA as control. The
439 sequences of the siRNAs are listed in Table S2.

440 *In vitro and in vivo EdU labeling:* For *in vitro* EdU labeling, EdU (APExBIO, B8337)
441 was supplemented in the culture medium for a final concentration of 20 mg/ml. Cells
442 were collected after 8 hours labeling.

443 For *in vivo* EdU labeling, mice were given an intraperitoneal injection with 50
444 mg/kg of EdU in sterile PBS for 8 consecutive days. After that, the animals were
445 sacrificed and the corneas were collected for cryosection. EdU signal in corneal
446 endothelium was detected using the Click-iT EdU Alexa Fluor 647 imaging kit
447 (Invitrogen, C10640) according to the manufacturer' s instruction.

448 *CCK-8 assay:* The CCK-8 solution (Vazyme, A311-01) was added to the culture
449 medium, and the absorbance value (450 nm) for each well was determined 2 hours
450 later using a microplate reader (Thermo, Multiskan GO).

451 *Western blot analysis：* Western blot analysis was performed as previously described.[47]
452 The equal amount of protein was resolved by SDS-PAGE and immunoblotted with
453 primary antibodies for YAP1 (Abclonal, A19134), phospho-YAP1-S127 (Abcam,
454 ab186735), LATS1/2 (Proteintech, 17049-1-AP), phospho-LATS1/2 (Thr1079)
455 (Proteintech, 28998-1-AP), MST1/2 (Proteintech, 22245-1-AP), phospho-MST1
456 (Thr183)/MST2 (Thr180) (Proteintech, 80093-1-RR), MOB1 (Proteintech,
457 11669-1-AP), phospho-MOB1 (Thr12) (Proteintech, 29027-1-AP) and β-actin
458 (Abcam, 8226). Primary antibodies were then detected with HRP-conjugated goat

459 anti-rabbit antibody (Abclonal, AS014), and the band intensity was semiquantified by
460 densitometry using ImageJ software and normalized by β-actin levels.
461 *Quantitative real-time polymerase chain reaction (qRT-PCR):* Total RNA was
462 extracted using Total RNA Extraction Reagent (Abclonal, RK30129), and cDNA was
463 made by using the RT Master Mix for qPCR (Abclonal, RK20433). Real-time qPCR
464 was performed with the SYBR Green qPCR Mix with UDG (Abclonal, RK21219),
465 and the primer sequences are listed in Table S3. The mixture was held at 37℃ for 2
466 min and then heated to 95℃ for 3 min, cycled 40 times (95℃ for 5 s, 60℃ for 30 s).
467 Melting curves were generated by increasing the temperature from 55℃ to 95℃ in
468 0.5℃ increments at 10 s intervals and then visually to ensure that a single peak was
469 present for each primer. Threshold amplification values (Ct) were assigned by the
470 LightCycler 96 analysis software (Roche).
471 *Immunofluorescence staining on cells and corneal whole mount:* Cells or corneas
472 were fixed with 4% paraformaldehyde for 20 min and incubated with 2% bovine
473 serum albumin for 60 min to reduce background noise. The cells or corneas were then
474 labeled with primary rabbit antibodies for YAP1 (Abclonal, A19134), Ki67 (Abcam,
475 ab16667), ZO-1 (Invitrogen, 61-7300) or Na^+-K^+ATPase (Abcam, ab76020) overnight
476 at 4℃. After 3 washes with PBS, the samples were incubated with goat anti-rabbit
477 lgG (Abclonal, AS053) for 120 min. The nuclei were stained with DAPI (Beyotime,
478 C1005) for 10 min. The samples were observed under a laser scanning confocal
479 microscopy (ZEISS, LSM880).
480 *Alizarin Red staining:* Mouse or rabbit corneas were incubated with Alizarin Red S
481 solution (Solarbio, G1452) for 5 min. After that, the corneas were fixed with 4%
482 paraformaldehyde for 20 min and cut into flat mount. Images were captured with a
483 microscope (Zeiss, Axio Lab.A1).
484 *Statistics:* Statistical analysis was performed using GraphPad Prism software 9.0.
485 Data were presented as mean±SEM and analyzed by unpaired Student's *t* test for two
486 groups and ANOVA for more than two groups. $P < 0.05$ was considered statistical
487 significant.
488 *Ethics Approval Statement:* The animal experiments were performed according to the
489 protocol approved by the Laboratory Animal Management and Ethics Committee of
490 Xiamen University (Approval No. XMULAC20240087).
491

Supporting Information

Supporting Information is available from the Wiley Online Library or from the author.

Acknowledgement

We thank Jingru Huang and Xiang You from Central Lab, School of Medicine, Xiamen University for technical support in confocal imaging. We thank Haiping Zheng from Central Lab, School of Medicine, Xiamen University for technical support in cell cycle analysis.

Conflict of interest:

The authors have declared that no conflict of interest exists.

Author contributions

J.Z., Y.G., H.Z. and W.L. designed the overall project and wrote the manuscript, J.Z., Y.G., H.Z., W.H., Y.W., M.Z., X.H., L.Z., J.Y. S.C. H.H. and R.Z. performed the experiments and data analysis. H.W. collected human corneoscleral tissues. Z.L., A.Q, C.C, and W.L. revised the manuscript. J.Z., Y.G., and H.Z. contributed equally to this work, thus should be considered as co-first authors. The order of co–first authors was decided by discussions among the 3 first authors and the 2 corresponding author. All authors have reviewed and approved the manuscript.

Data Availability Statement

The data supporting the findings of this study are available in the Supporting Data Values file. The raw data used in this study are available from the corresponding author upon reasonable request.

References

[1] K.M. Meek, C. Knupp, Corneal structure and transparency, Prog Retin Eye Res, 49 (2015) 1–16.

[2] G. Suanno, V.G. Genna, E. Maurizi, A. Abu Dieh, M. Griffith, G. Ferrari, Cell therapy in the cornea: The emerging role of microenvironment, Prog Retin Eye Res, 102 (2024).

523 [3] W.M. Bourne, Biology of the corneal endothelium in health and disease, Eye, 17 (2003)
524 912–918.
525 [4] K. Gupta, S.X. Deng, Corneal Endothelial Decompensation, Klin Monatsbl Augenh, 237 (2020)
526 745–753.
527 [5] Z.G. He, N. Campolmi, P. Gain, M.H. Binh, J.M. Dumollard, S. Duband, M. Peoc'h, S. Piselli,
528 O. Garraud, G. Thuret, Revisited Microanatomy of the Corneal Endothelial Periphery: New
529 Evidence for Continuous Centripetal Migration of Endothelial Cells in Humans, Stem Cells, 30
530 (2012) 2523–2534.
531 [6] X. Zhang, H. Liu, C. Wan, Y. Li, C. Ren, J. Lu, Y. Liu, Y. Yang, Verteporfin combined with
532 ROCK inhibitor promotes the restoration of corneal endothelial cell dysfunction in rats, Biochem
533 Pharmacol, 231 (2025) 116641.
534 [7] A. Viberg, B. Samolov, B. Bystroem, Descemet Stripping Automated Endothelial Keratoplasty
535 versus Descemet Membrane Endothelial Keratoplasty for Fuchs Endothelial Corneal Dystrophy,
536 Ophthalmology, 130 (2023) 1248–1257.
537 [8] M.O. Price, P. Calhoun, C. Kollman, F.W. Price, J.H. Lass, Descemet Stripping Endothelial
538 Keratoplasty, Ophthalmology, 123 (2016) 1421–1427.
539 [9] S. Kinoshita, N. Koizumi, M. Ueno, N. Okumura, K. Imai, H. Tanaka, Y. Yamamoto, T.
540 Nakamura, T. Inatomi, J. Bush, M. Toda, M. Hagiya, I. Yokota, S. Teramukai, C. Sotozono, J.
541 Hamuro, Injection of Cultured Cells with a ROCK Inhibitor for Bullous Keratopathy, New Engl J
542 Med, 378 (2018) 995–1003.
543 [10] K. Numa, K. Imai, M. Ueno, K. Kitazawa, H. Tanaka, J.D. Bush, S. Teramukai, N. Okumura,
544 N. Koizumi, J. Hamuro, C. Sotozono, S. Kinoshita, Five-Year Follow-up of First 11 Patients
545 Undergoing Injection of Cultured Corneal Endothelial Cells for Corneal Endothelial Failure,
546 Ophthalmology, 128 (2021) 504–514.
547 [11] Z.Y. Li, H.Y. Duan, Y.N. Jia, C. Zhao, W.J. Li, X. Wang, Y.J. Gong, C.X. Dong, B.C. Ma, S.Q.
548 Dou, B. Zhang, D.F. Li, Y.H. Cao, L.X. Xie, Q.J. Zhou, W.Y. Shi, Long-term corneal recovery by
549 simultaneous delivery of hPSC-derived corneal endothelial precursors and nicotinamide, J Clin
550 Invest, 132 (2022).
551 [12] N. Okumura, S. Nakano, E.P. Kay, R. Numata, A. Ota, Y. Sowa, T. Sakai, M. Ueno, S.
552 Kinoshita, N. Koizumi, Involvement of Cyclin D and p27 in Cell Proliferation Mediated by

553 ROCK Inhibitors Y-27632 and Y-39983 During Corneal Endothelium Wound Healing, Invest
554 Ophth Vis Sci, 55 (2014) 318–329.
555 [13] L.C. Meekins, N. Rosado-Adames, R. Maddala, J.J. Zhao, P.V. Rao, N.A. Afshari, Corneal
556 Endothelial Cell Migration and Proliferation Enhanced by Rho Kinase (ROCK) Inhibitors in In
557 Vitro and In Vivo Models, Invest Ophth Vis Sci, 57 (2016) 6731–6738.
558 [14] N. Okumura, Y. Okazaki, R. Inoue, K. Kakutani, S. Nakano, S. Kinoshita, N. Koizumi, Effect
559 of the Rho-Associated Kinase Inhibitor Eye Drop (Ripasudil) on Corneal Endothelial Wound
560 Healing, Invest Ophth Vis Sci, 57 (2016) 1284–1292.
561 [15] H. Miyagi, S. Kim, J. Li, C.J. Murphy, S.M. Thomasy, Topical Rho-Associated Kinase
562 Inhibitor, Y27632, Accelerates Corneal Endothelial Regeneration in a Canine Cryoinjury Model,
563 Cornea, 38 (2019) 352–359.
564 [16] N. Koizumi, N. Okumura, M. Ueno, H. Nakagawa, J. Hamuro, S. Kinoshita, Rho-Associated
565 Kinase Inhibitor Eye Drop Treatment as a Possible Medical Treatment for Fuchs Corneal
566 Dystrophy, Cornea, 32 (2013) 1167–1170.
567 [17] G. Moloney, C. Petsoglou, M. Ball, Y. Kerdraon, R. Höllhumer, N. Spiteri, S. Beheregaray, J.
568 Hampson, M. D'Souza, R.N. Devasahayam, Descemetorhexis Without Grafting for Fuchs
569 Endothelial Dystrophy-Supplementation With Topical Ripasudil, Cornea, 36 (2017) 642–648.
570 [18] N. Okumura, S. Kinoshita, N. Koizumi, Application of Rho Kinase Inhibitors for the
571 Treatment of Corneal Endothelial Diseases, J Ophthalmol, 2017 (2017).
572 [19] W.D. Pei, J. Chen, W.Y. Wu, W. Wei, Y. Yu, Y. Feng, Comparison of the rabbit and human
573 corneal endothelial proteomes regarding proliferative capacity, Exp Eye Res, 209 (2021).
574 [20] K. Yoshida, S. Kase, K. Nakayama, H. Nagahama, T. Harada, H. Ikeda, C. Harada, J. Imaki,
575 K. Ohgami, K. Shiratori, I.B. Ilieva, S. Ohno, S. Nishi, K.I. Nakayama, Involvement of p27 in the
576 proliferation of the developing corneal endothelium, Invest Ophth Vis Sci, 45 (2004) 2163–2167.
577 [21] S.P. Hui, D.Z. Sheng, K. Sugimoto, A. Gonzalez-Rajal, S. Nakagawa, D. Hesselson, K.
578 Kikuchi, Zebrafish Regulatory T Cells Mediate Organ-Specific Regenerative Programs, Dev Cell,
579 43 (2017) 659–+.
580 [22] P. Lyu, M. Iribarne, D. Serjanov, Y.J. Zhai, T. Hoang, L.J. Campbell, P. Boyd, I. Palazzo, M.
581 Nagashima, N.J. Silva, P.F. Hitchcock, J. Qian, D.R. Hyde, S. Blackshaw, Common and divergent

582 gene regulatory networks control injury-induced and developmental neurogenesis in zebrafish
583 retina, Nat Commun, 14 (2023).
584 [23] L. Celotto, F. Rost, A. Machate, J. Bläsche, A. Dahl, A. Weber, S. Hans, M. Brand, Single-cell
585 RNA sequencing unravels the transcriptional network underlying zebrafish retina regeneration,
586 Elife, 12 (2023).
587 [24] A. Elbediwy, Z.I. Vincent-Mistiaen, B. Spencer-Dene, R.K. Stone, S. Boeing, S.K. Wculek, J.
588 Cordero, E.H. Tan, R. Ridgway, V.G. Brunton, E. Sahai, H. Gerhardt, A. Behrens, I. Malanchi, O.J.
589 Sansom, B.J. Thompson, Integrin signalling regulates YAP and TAZ to control skin homeostasis,
590 Development, 143 (2016) 1674–1687.
591 [25] Z. Liu, H. Wu, K. Jiang, Y. Wang, W. Zhang, Q. Chu, J. Li, H. Huang, T. Cai, H. Ji, C. Yang,
592 N. Tang, MAPK-Mediated YAP Activation Controls Mechanical-Tension-Induced Pulmonary
593 Alveolar Regeneration, Cell Rep, 16 (2016) 1810–1819.
594 [26] M. Xin, Y. Kim, L.B. Sutherland, M. Murakami, X.X. Qi, J. McAnally, E.R. Porrello, A.I.
595 Mahmoud, W. Tan, J.M. Shelton, J.A. Richardson, H.A. Sadek, R. Bassel-Duby, E.N. Olson,
596 Hippo pathway effector Yap promotes cardiac regeneration, P Natl Acad Sci USA, 110 (2013)
597 13839–13844.
598 [27] L. Lu, Y. Li, S.M. Kim, W. Bossuyt, P. Liu, Q. Qiu, Y. Wang, G. Halder, M.J. Finegold, J.S.
599 Lee, R.L. Johnson, Hippo signaling is a potent in vivo growth and tumor suppressor pathway in
600 the mammalian liver, Proc Natl Acad Sci U S A, 107 (2010) 1437–1442.
601 [28] F.X. Yu, K.L. Guan, The Hippo pathway: regulators and regulations, Gene Dev, 27 (2013)
602 355–371.
603 [29] J.B. Huang, S. Wu, J. Barrera, K. Matthews, D.J. Pan, The Hippo signaling pathway
604 coordinately regulates cell proliferation and apoptosis by inactivating Yorkie, the homolog of YAP,
605 Cell, 122 (2005) 421–434.
606 [30] A. Perra, M.A. Kowalik, E. Ghiso, G.M. Ledda-Columbano, L. Di Tommaso, M.M. Angioni,
607 C. Raschioni, E. Testore, M. Roncalli, S. Giordano, A. Columbano, YAP activation is an early
608 event and a potential therapeutic target in liver cancer development, J Hepatol, 61 (2014)
609 1088–1096.
610 [31] F.Q. Fan, Z.X. He, L.L. Kong, Q.H. Chen, Q. Yuan, S.H. Zhang, J.J. Ye, H. Liu, X.F. Sun, J.
611 Geng, L.Z. Yuan, L.X. Hong, C. Xiao, W.J. Zhang, X.H. Sun, Y.Z. Li, P. Wang, L.H. Huang, X.R.

612 Wu, Z.L. Ji, Q. Wu, N.S. Xia, N.S. Gray, L.F. Chen, C.H. Yun, X.M. Deng, D.W. Zhou,
613 Pharmacological targeting of kinases MST1 and MST2 augments tissue repair and regeneration,
614 Sci Transl Med, 8 (2016).
615 [32] Y.T. Zhu, H.C. Chen, S.Y. Chen, S.C.G. Tseng, Nuclear p120 catenin unlocks mitotic block of
616 contact-inhibited human corneal endothelial monolayers without disrupting adherent junctions, J
617 Cell Sci, 125 (2012) 3636–3648.
618 [33] C. Zhao, Q.J. Zhou, H.Y. Duan, X. Wang, Y.N. Jia, Y.J. Gong, W.J. Li, C.X. Dong, Z.Y. Li,
619 W.Y. Shi, Laminin 511 Precoating Promotes the Functional Recovery of Transplanted Corneal
620 Endothelial Cells, Tissue Eng Pt A, 26 (2020) 1158–1168.
621 [34] Y.J. Hsueh, H.C. Chen, S.E. Wu, T.K. Wang, J.K. Chen, D.H.K. Ma, Lysophosphatidic acid
622 induces YAP-promoted proliferation of human corneal endothelial cells via PI3K and ROCK
623 pathways, Mol Ther-Meth Clin D, 2 (2015).
624 [35] J. Chen, Z. Li, L. Zhang, S. Ou, Y. Wang, X. He, D. Zou, C. Jia, Q. Hu, S. Yang, X. Li, J. Li, J.
625 Wang, H. Sun, Y. Chen, Y.T. Zhu, S.C.G. Tseng, Z. Liu, W. Li, Descemet's Membrane Supports
626 Corneal Endothelial Cell Regeneration in Rabbits, Sci Rep, 7 (2017) 6983.
627 [36] I.M. Moya, G. Halder, Hippo-YAP/TAZ signalling in organ regeneration and regenerative
628 medicine, Nat Rev Mol Cell Bio, 20 (2019) 211–226.
629 [37] N. Kastan, K. Gnedeva, T. Alisch, A.A. Petelski, D.J. Huggins, J. Chiaravalli, A. Aharanov, A.
630 Shakked, E. Tzahor, A. Nagiel, N. Segil, A.J. Hudspeth, Small-molecule inhibition of Lats kinases
631 may promote Yap-dependent proliferation in postmitotic mammalian tissues, Nat Commun, 12
632 (2021).
633 [38] L.R. Fiedler, K. Chapman, M. Xie, E. Maifoshie, M. Jenkins, P.A. Golforoush, M. Bellahcene,
634 M. Noseda, D. Faust, A. Jarvis, G. Newton, M.A. Paiva, M. Harada, D.J. Stuckey, W.H. Song, J.
635 Habib, P. Narasimham, R. Aqil, D. Sanmugalingam, R. Yan, L. Pavanello, M. Sano, S.C. Wang,
636 R.D. Sampson, S. Kanayaganam, G.E. Taffet, L.H. Michae, M.L. Entman, T.H. Tan, S.E. Harding,
637 C.M.R. Low, C. Tralau-Stewart, T. Perrior, M.D. Schneider, MAP4K4 Inhibition Promotes
638 Survival of Human Stem Cell-Derived Cardiomyocytes and Reduces Infarct Size, Cell Stem Cell,
639 24 (2019) 579–+.
640 [39] A. Ocampo, P. Reddy, P. Martinez-Redondo, A. Platero-Luengo, F. Hatanaka, T. Hishida, M.
641 Li, D. Lam, M. Kurita, E. Beyret, T. Araoka, E. Vazquez-Ferrer, D. Donoso, J.L. Roman, J. Xu, C.

642 Rodriguez Esteban, G. Nuñez, E. Nuñez Delicado, J.M. Campistol, I. Guillen, P. Guillen, J.C.
643 Izpisua Belmonte, In Vivo Amelioration of Age-Associated Hallmarks by Partial Reprogramming,
644 Cell, 167 (2016) 1719–1733.e1712.
645 [40] D. Yimlamai, C. Christodoulou, G.G. Galli, K. Yanger, B. Pepe-Mooney, B. Gurung, K.
646 Shrestha, P. Cahan, B.Z. Stanger, F.D. Camargo, Hippo pathway activity influences liver cell fate,
647 Cell, 157 (2014) 1324–1338.
648 [41] M. Xin, Y. Kim, L.B. Sutherland, M. Murakami, X. Qi, J. McAnally, E.R. Porrello, A.I.
649 Mahmoud, W. Tan, J.M. Shelton, J.A. Richardson, H.A. Sadek, R. Bassel-Duby, E.N. Olson,
650 Hippo pathway effector Yap promotes cardiac regeneration, Proc Natl Acad Sci U S A, 110 (2013)
651 13839–13844.
652 [42] J.H. Bu, J.W. Yu, Y. Wu, X.X. Cai, K.C. Li, L.Y. Tang, N. Jiang, M.V. Jeyalatha, M.J. Zhang,
653 H.M. Sun, H. He, A.J. Quantock, Y.X. Chen, Z.G. Liu, W. Li, Hyperlipidemia Affects Tight
654 Junctions and Pump Function in the Corneal Endothelium, Am J Pathol, 190 (2020) 563–576.
655 [43] N. Okumura, N. Koizumi, E.P. Kay, M. Ueno, Y. Sakamoto, S. Nakamura, J. Hamuro, S.
656 Kinoshita, The ROCK Inhibitor Eye Drop Accelerates Corneal Endothelium Wound Healing,
657 Invest Ophth Vis Sci, 54 (2013) 2493–2502.
658 [44] C.L. Liu, T. Miyajima, G. Melangath, T. Miyai, S. Vasanth, N. Deshpande, V. Kumar, S.O.
659 Tone, R. Gupta, S. Zhu, D. Vojnovic, Y.M. Chen, E.G. Rogan, B. Mondal, M. Zahid, U.V.
660 Jurkunas, Ultraviolet A light induces DNA damage and estrogen-DNA adducts in Fuchs
661 endothelial corneal dystrophy causing females to be more affected, P Natl Acad Sci USA, 117
662 (2020) 573–583.
663 [45] C. Zhao, W. Li, H. Duan, Z. Li, Y. Jia, S. Zhang, X. Wang, Q. Zhou, W. Shi, NAD(+)
664 precursors protect corneal endothelial cells from UVB-induced apoptosis, Am J Physiol Cell
665 Physiol, 318 (2020) C796–c805.
666 [46] W. Li, A.L. Sabater, Y.T. Chen, Y. Hayashida, S.Y. Chen, H. He, S.C.G. Tseng, A novel
667 method of isolation, preservation, and expansion of human corneal endothelial cells, Invest Ophth
668 Vis Sci, 48 (2007) 614–620.
669 [47] S. Li, L. Tang, J. Zhou, S. Anchouche, D. Li, Y. Yang, Z. Liu, J. Wu, J. Hu, Y. Zhou, J. Yin, Z.
670 Liu, W. Li, Sleep deprivation induces corneal epithelial progenitor cell over-expansion through
671 disruption of redox homeostasis in the tear film, Stem Cell Reports, 17 (2022) 1105–1119.